AFRL-VA-WP-TR-1999-3086

IMPROVEMENT AND VALIDATION OF THE COMPUTATIONAL AEROELASTICITY CODE ENS3DAE

DEAN HAWKINSON

AFRL/VASD
2130 EIGHTH STREET
SUITE 1
WRIGHT-PATTERSON AFB, OH 45433-7542

SEPTEMBER 1999

FINAL REPORT FOR 07/05/1994 – 08/31/1998

APPROVED FOR PUBLIC RELEASE; DISTRIBUTION UNLIMITED

AIR VEHICLES DIRECTORATE
AIR FORCE RESEARCH LABORATORY
AIR FORCE MATERIEL COMMAND
WRIGHT-PATTERSON AIR FORCE BASE OH 45433-7542

This technical report has been reviewed and is approved for publication.

L J Huttsell

for Dean Hawkinson
Co-op Student
Structural Design and Development Branch

L J Huttsell

L. J. HUTTSELL
Aeroelasticity Team Leader
Structural Design and Development Branch

Nelson D. Wolf

NELSON D. WOLF
Chief, Structural Design and Development Branch
Structures Division

REPORT DOCUMENTATION PAGE			Form Approved OMB No. 0704-0188

1. AGENCY USE ONLY *(Leave blank)*	2. REPORT DATE	3. REPORT TYPE AND DATES COVERED
	SEPTEMBER 1999	FINAL REPORT FOR 01/04/99 THROUGH 01/07/99

4. TITLE AND SUBTITLE
Improvement and Validation of the Computational Aeroelasticity Code ENS3DAE

5. FUNDING NUMBERS
C In-house
PE 62201
PR 2401
TA LE
WU 00

6. AUTHOR(S)
DEAN HAWKINSON

7. PERFORMING ORGANIZATION NAME(S) AND ADDRESS(ES)
AFRL/VASD
2130 EIGHTH STREET, SUITE 1
WRIGHT-PATTERSON AFB, OH 45433-7542

8. PERFORMING ORGANIZATION REPORT NUMBER

9. SPONSORING/MONITORING AGENCY NAME(S) AND ADDRESS(ES)
AIR VEHICLES DIRECTORATE
AIR FORCE RESEARCH LABORATORY
AIR FORCE MATERIEL COMMAND
WRIGHT-PATTERSON AFB, OH 45433-7542
POC: LARRY HUTTSELL, AFRL/VASD, 937-255-8456

10. SPONSORING/MONITORING AGENCY REPORT NUMBER
AFRL-VA-WP-TR-1999-3086

11. SUPPLEMENTARY NOTES
This report was generated by Co-op student Dean Hawkinson of Iowa State University during his employment at AFRL/VASD.

12a. DISTRIBUTION AVAILABILITY STATEMENT
Approved for public release; distribution unlimited.

12b. DISTRIBUTION CODE

13. ABSTRACT *(Maximum 200 words)*
The heightened awareness of the importance of fluid-structures interaction has lead to the development of several tools for addressing such issues. One continually developing tool, ENS3DAE has been adopted for use by several researchers and engineers. In the interest of increased generality, additional capabilities have been implemented into the software. Of these new improvements, the ability to generate a static aeroelastic solution to a two-dimensional airfoil problem using different grid topologies has been successfully completed.

Originally written to use H-type grids, ENS3DAE was not able to aeroelastically deflect the two degree of freedom airfoil. After small logic modifications and adjusting a standard input file, a reasonable static aeroelastic solution was obtained. Future plans include validation of the current work and development of a dynamic aeroelastic, pitch & plunge case for the NACA 64A006 airfoil.

14. SUBJECT TERMS
2-D AIRFOIL, CFD, AEROELASTIC

15. NUMBER OF PAGES
12

16. PRICE CODE

17. SECURITY CLASSIFICATION OF REPORT	18. SECURITY CLASSIFICATION OF THIS PAGE	19. SECURITY CLASSIFICATION OF ABSTRACT	20. LIMITATION OF ABSTRACT
UNCLASSIFIED	UNCLASSIFIED	UNCLASSIFIED	SAR

TABLE OF CONTENTS

LIST OF FIGURES

LIST OF TABLES

1. Summary

Developed under contract for the Air Force Research Laboratory at Lockheed Martin, ENS3DAE (Euler/Navier-Stokes 3-Dimensional AEroelastic) is a multi-functional computational aeroelasticity code. It is capable of developing solutions to a wide range of problems.

Because Computational Fluid Dynamics relies on the discretization of partial differential equations into finite difference algebraic equations solved over a grid, it is important to examine the behaviors of different grid shapes and their effect on the final solution. This report covers three grid topologies that are common in aerospace applications, C-, O- and H- grids.

Because ENS3DAE was developed for generality, the authors felt the H-grid would be most practical for aeroelastic applications. For this reason, much of the logic used in the aeroelastic routines is specific to H-grid characteristics.

Unfortunately, for many applications, H-type grids are less suited than C- and O-. Examples include the use of O-grids for cylinder applications and C-grids for airfoil configurations.

The problem being addressed in this report is the classic 2 DOF airfoil flutter model. It was modeled within a 3D computational domain by using symmetry planes at the root and tip, essentially simulating an infinitely long rectangular wing.

As a delivered package, pre-release version 5.4 was not capable of handling aeroelastic deflection of an airfoil model using the C- and O- grids. After examining the internal logic, changes were made to the code that allows this type of problem to be solved. Following other insights, a static aeroelastic solution was attained.

After comparing the results from the three topologies, several conclusions can be drawn. The first is that the minor modifications to the software allow the successful simulation of the static aeroelastic 2 DOF airfoil.

2. Introduction

The introduction of flexible structures into medium and high fidelity Computational Fluid Dynamics (CFD) codes has received attention recently. The increased performance of computers has allowed the solution of fully coupled fluid/structures problems. ENS3DAE is an example of a developing tool for creating solutions to these problems. Developed under contract for the Air Force Research Laboratory, Air Vehicles Directorate, ENS3DAE has integrated many of the new technologies and methodologies for solving three-dimensional fluid problems while incorporating structural flexibility.

As with most CFD programs, ENS3DAE has the ability to solve problems of various A/C configurations. This document will discuss how allowing aeroelastic solution using three grid topologies has enhanced this ability. The discussion will cover the process from grid construction to code modification and testing, as well as discuss results for a 2-degree of freedom Pitch/Plunge airfoil problem.

In addition to creating the enhanced capabilities, the report will discuss how other newly implemented code modifications were examined for their validity. Including a new solution algorithm and several differencing and dissipation options, we will discuss how these options perform.

This is documentation of the technical work done by the author (an undergraduate student from Iowa State University near completion of the degree program in aerospace engineering). The work was performed within the Design & Analysis Branch of the Air Vehicles-Structures Division at the Air Force Research Laboratory. This report will discuss the contributions that the author made and characterize the benefit of the experience on his educational goals.

3. Motivation

As the title of this project suggests, the motivation for performing this work was to increase the capabilities of ENS3DAE while examining the validity of new software capabilities. ENS3DAE was selected because of its wide use within the computational aeroelastic community. Specifically, the Aerodynamics, Structures and Controls Integration (ASCI) steering committee chose ENS3DAE as one of the codes for work of this type.

The ASCI steering committee is a multi-disciplinary team headed by industry. It is made up of representatives from the aerospace industry, government, and academia. Their goal is to roadmap multidisciplinary design and analysis issues to utilize resources from all of the diversity of the aerospace community.

4. Procedure

In order to generate the static-aeroelastic solution for the given problem, several steps were needed. The NACA 64A006 airfoil was selected because of its relative familiarity and availability of comparison studies. Several steps that would typically be necessary to conduct this type of study were unnecessary because of the previous work.

The previous aeroelasticity work with the NACA 64A006 airfoil allowed the focus of this study to remain on improving ENS3DAE for other grid topologies. The first step was to create three comparable grids, one of each of the mentioned topologies.

Following the successful generation of a static-rigid flow solution, initial attempts were made at static-aeroelastic. With this, the modifications to the code and input file were generated.

5. Results

Before generating the computational grid, a database for geometry definition needs to be created.

After examining results using the standard AGARD airfoil definition for NACA 64A006, a somewhat modified version was used.

NACA 64A006
Upper Surface Definition
AGARD Report #R702

X coordinate	Y coordinate
0.0000	0.00000
0.0005	0.00158
0.0010	0.00221
0.0015	0.00270
0.0020	0.00311
0.0025	0.00347
0.0030	0.00379
0.0035	0.00409
0.0040	0.00435
0.0050	0.00485
0.0075	0.00585
0.0125	0.00739
0.0250	0.01016
0.0500	0.01399
0.0750	0.01684
0.1000	0.01919
0.1500	0.02283
0.2000	0.02557
0.2500	0.02757
0.3000	0.02896
0.3500	0.02977
0.4000	0.02999
0.4500	0.02945
0.5000	0.02825
0.5500	0.02653
0.6000	0.02438
0.6500	0.02188
0.7000	0.01907
0.7500	0.01602
0.8000	0.01285
0.8500	0.00967
0.9000	0.00649
0.9500	0.00331
1.0000	0.00000

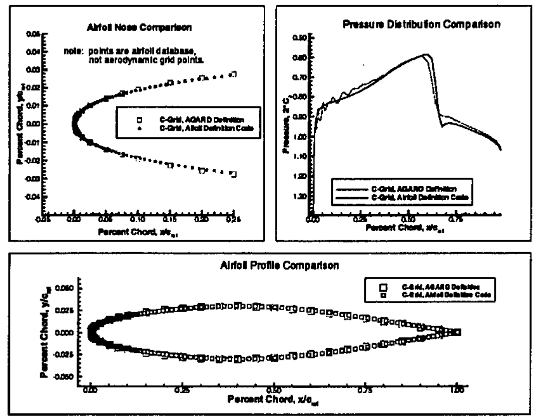

Figure 1. Effect of Geometry Definition on the Aerodynamic Solution.

Initial attempts to model the NACA 64A006 airfoil made use of AGARD Report # R702. After creating the computational grid using the AGARD definition, the AGARD data was identified to be inadequately refined.

The computational grid was generated with the GridGen modeling package. This software uses linear splines between data points, creating a jagged model of the airfoil.

To avoid this problem, a relatively undocumented program was used to generate the airfoil data set. A table of points is included to provide for duplication of the geometry used for this study. The AGARD data set has also been included for comparison.

Table 2. NACA 64A006m Upper Surface Definition (Airfoil Definition Code)

X coordinate	Y coordinate
0.000000E+00	0.000000E+00
2.600000E-05	3.592568E-04
1.070000E-04	7.264749E-04
2.530000E-04	1.113298E-03
4.730000E-04	1.516792E-03
7.820000E-04	1.942852E-03
1.188000E-03	2.385094E-03
1.702000E-03	2.842883E-03
2.334000E-03	3.314650E-03
3.093000E-03	3.798548E-03
3.987000E-03	4.292702E-03
5.024000E-03	4.795760E-03
6.209000E-03	5.305459E-03
7.549000E-03	5.820963E-03
9.049000E-03	6.340934E-03
1.071400E-02	6.864389E-03
1.255000E-02	7.390854E-03
1.456100E-02	7.919434E-03
1.675200E-02	8.449680E-03
1.913000E-02	8.981671E-03
2.170000E-02	9.515033E-03
2.447000E-02	1.005003E-02
2.744500E-02	1.058631E-02
3.063400E-02	1.112427E-02
3.404300E-02	1.166372E-02
3.768200E-02	1.220510E-02
4.155900E-02	1.274846E-02
4.568200E-02	1.329386E-02
5.006200E-02	1.384167E-02
5.470700E-02	1.439188E-02
5.962800E-02	1.494476E-02
6.483500E-02	1.550044E-02
7.033900E-02	1.605910E-02
7.614900E-02	1.662067E-02
8.227700E-02	1.718533E-02
8.873399E-02	1.775312E-02
9.552899E-02	1.832382E-02
1.026730E-01	1.889738E-02
1.101770E-01	1.947360E-02
1.180510E-01	2.005219E-02
1.263050E-01	2.063273E-02
1.349470E-01	2.121455E-02
1.439870E-01	2.179703E-02
1.534330E-01	2.237924E-02
1.632920E-01	2.296004E-02
1.735700E-01	2.353806E-02
1.842740E-01	2.411177E-02
1.954080E-01	2.467923E-02
2.069740E-01	2.523816E-02
2.189750E-01	2.578605E-02
2.314120E-01	2.631997E-02
2.442830E-01	2.683652E-02
2.575850E-01	2.733191E-02
2.713150E-01	2.780199E-02
2.854660E-01	2.824207E-02
3.000300E-01	2.864700E-02
3.149970E-01	2.901121E-02
3.303550E-01	2.932868E-02
3.460900E-01	2.959299E-02
3.621860E-01	2.979728E-02
3.786250E-01	2.993439E-02
3.953870E-01	2.999690E-02
4.124510E-01	2.997757E-02
4.297920E-01	2.987318E-02
4.473850E-01	2.968329E-02
4.652030E-01	2.940824E-02
4.832180E-01	2.904911E-02
5.014000E-01	2.860773E-02
5.197180E-01	2.808668E-02
5.381400E-01	2.748926E-02
5.566340E-01	2.681937E-02
5.751670E-01	2.608157E-02
5.937040E-01	2.528101E-02
6.122140E-01	2.442310E-02
6.306630E-01	2.351381E-02
6.490180E-01	2.255934E-02
6.672470E-01	2.156607E-02
6.853189E-01	2.054051E-02
7.032040E-01	1.948915E-02
7.208730E-01	1.841844E-02
7.382990E-01	1.733463E-02
7.554559E-01	1.624381E-02
7.723199E-01	1.515173E-02
7.888690E-01	1.406381E-02
8.050820E-01	1.298512E-02
8.209420E-01	1.192856E-02
8.364310E-01	1.089670E-02
8.515359E-01	9.890435E-03
8.662440E-01	8.910609E-03
8.805459E-01	7.957836E-03
8.944319E-01	7.032770E-03
9.078980E-01	6.135686E-03
9.209390E-01	5.266915E-03
9.335500E-01	4.426792E-03
9.457290E-01	3.615446E-03
9.574890E-01	2.832014E-03
9.688310E-01	2.076429E-03
9.797090E-01	1.351752E-03
9.900960E-01	6.597908E-04
1.000000E+00	0.000000E+00

Using the geometry definitions given, the C-, H- and O- type grids were created with GridGen. The H- grid is made up of two rectangular zones. The C- and O- grids are made from a single zone, wrapped around the airfoil geometry. It is also clear how the C-grid is considered a hybrid of H- and O-. An important concern when generating the grids was to ensure that they were similar.

The similarities include; distance to far-field boundaries, number of grid points on airfoil surfaces, grid spacing at the leading and trailing edges and the distance from the airfoil to first grid point in the normal direction. Additional similarities exist that were implemented to allow for valid comparisons.

Common Characteristics:
Distance to far-field boundaries: 10 units.
Number of grid points on airfoil: 200,
100 upper and 100 lower.
Grid spacing at Leading Edge: 0.0025 units.
Grid spacing at Trailing Edge: 0.01 units.

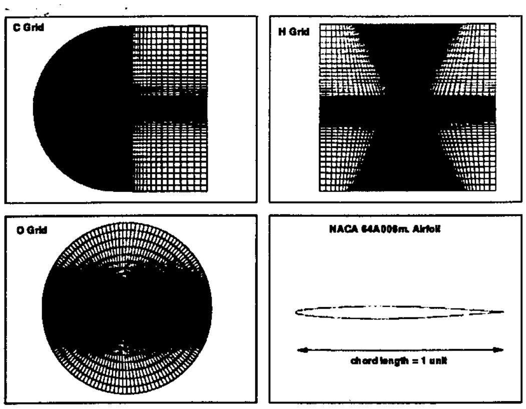

Figure 2. The C-, H-, and O- Grids

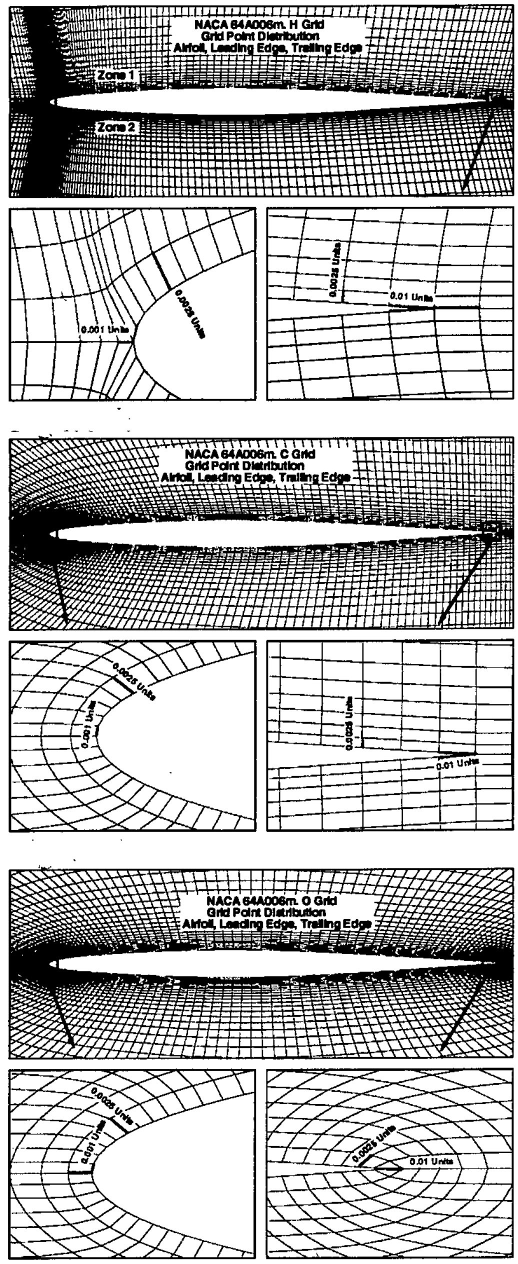

Figures 3-5. Characterization of the Similarities between the Three Grids

The figures also demonstrate the advantages of using C- grids for airfoil geometry. Notice the skewed grid lines at the leading edge in the H- grid and the trailing edge for the O-. These skewed areas introduce problems to the numerical methods used to solve the standard flow equations.

For the remainder of this discussion, it is assumed that the reader has some familiarity with ENS3DAE. Documentation included with the code provides information that is more than adequate.

5.1 STATIC – RIGID STEADY-STATE

Although ENS3DAE has the ability to treat the wing as a flexible structure, a good starting point is for a non-moving, rigid wing. ENS3DAE also has two methods for treating time in the aerodynamic solution. The steady-state setting advances the solution at the fastest appropriate time for each grid cell.

The purpose of generating the static-rigid solution was to benchmark ENS3DAE capabilities. It was observed that the different grid topologies caused little difficulty in this configuration.

Besides dissipation issues, the following figures illustrate the pressure fields surrounding the NACA airfoil at zero aoa and 0.87 Mach.

Figure 6 illustrates a problem that will resurface in further study. The 'hook' at the trailing edge of the pressure distribution for the O-grid is caused by the nature of the geometry. A detailed discussion will be covered in the Recommendations. Figure 7 shows the convergence of this solution.

In the figures that follow, all runs were made with the default settings. The authors of ENS3DAE were successful in making this type of run quite simple. Special consideration is needed when setting up the boundary conditions, however. These are covered within the section titled, "Static-Rigid, Steady-state, Special Considerations."

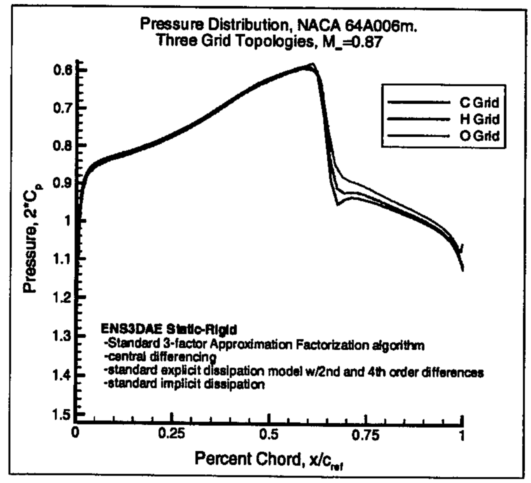

Figure 6. Pressure Distribution on the Airfoil Calculated with Default Settings for the Three Grids

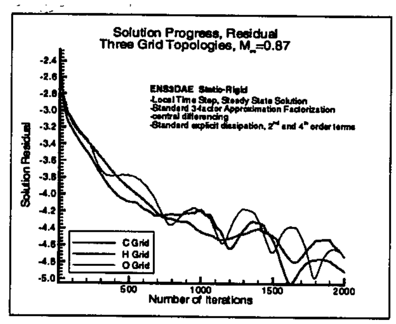

Figure 7. Convergence of the Solution

5.2 STATIC-RIGID TIME ACCURATE

Users of ENS3DAE also have options to run in a time accurate mode. In this setting, the solution is advanced at the largest time step that will be stable for the entire domain. A disadvantage of this setting is the slower convergence. The user is required to allow for more iterations to attain a satisfactory solution.

The work done as part of this project using the time accurate setting has raised some issues for future investigation.

The following figures (Figures 8 and 9) will demonstrate that the steady state and time accurate solutions converge to different solutions. For the purposes of this study, only a comparison of the results was necessary. Close examination shows that they show a slightly different shock location. However, the issue should be resolved before attempting to generate a dynamic-aeroelastic solution of the 2 DOF airfoil.

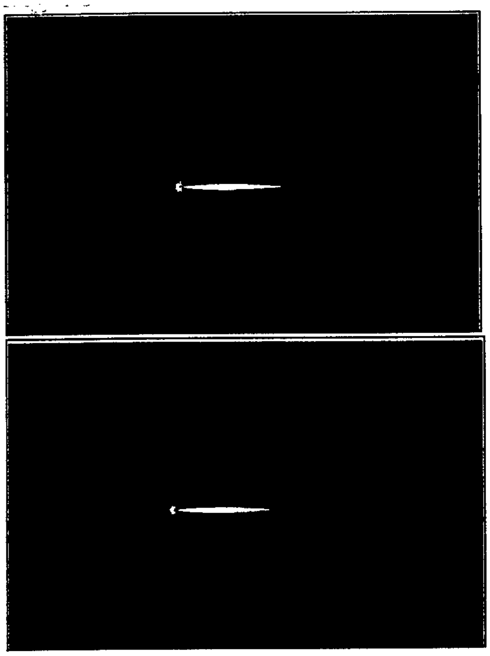

Figure 8. Pressure Distribution for both the Steady State (top) and the Time Accurate (bottom) settings

Several hypotheses have been put forth to explain the differences between the solutions. Because of time issues, a more thorough examination of each will be future work. A possible cure is a hybrid approach consisting of the steady state for a specific duration then restarting the solution with the time accurate model.

Figure 10 represents work that was meant to validate additional algorithm settings that were implemented in the latest release of ENS3DAE. It was hoped that these algorithm and dissipation options would shed light on the time accurate issues.

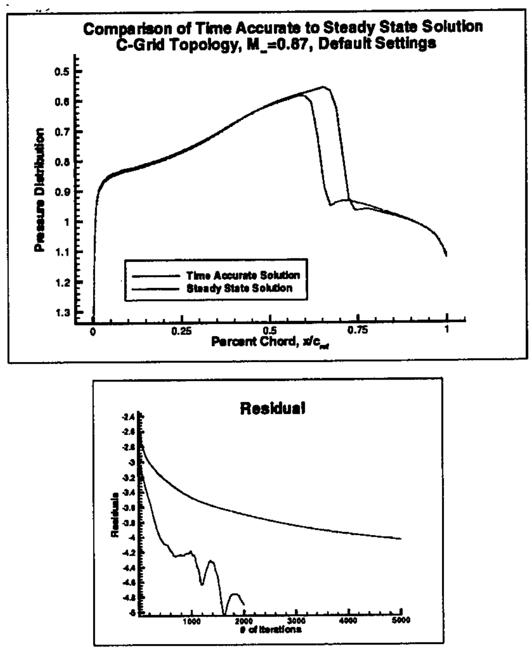

Figure 9. Difference in Shock Location Between Time Accurate and Steady State Settings

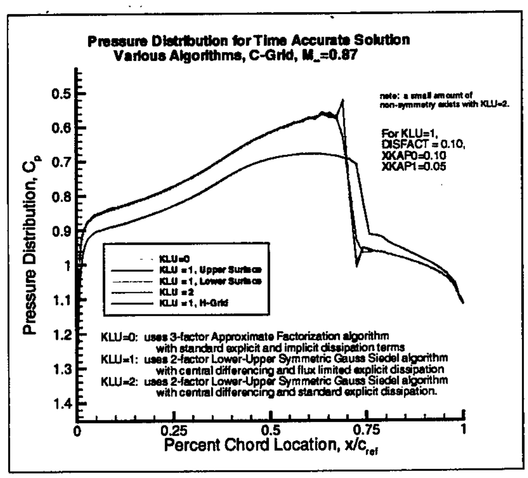

Figure 10. Issues Regarding New Algorithm and Dissipation/Differencing Models

Table 3: Static-Rigid Cases/Results

Steady – State	Default Conditions	H – Grid	Good results
		O – Grid	Good, Slightly over damped
		C – Grid	Good, Slightly under damped
	TVD = 1 Recommended	C – Grid	Good, better than Default
Time Accurate	Default Conditions	H – Grid	Good Results, different than S-S
		O – Grid	Good Results, different than S-S
		C – Grid	Good Results, different than S-S
	KLU = 1 Recommended	H – Grid	Not converged, but symmetric. Appears to be approaching default
		C – Grid	Large oscillations at shock, Non-symmetric upper/lower airfoil surface.
	KLU = 1 Increased damping	C – Grid	Little or no improvement, Non-symmetric upper/lower airfoil surfaces.
	KLU = 2	C – Grid	Good solution matches well with default settings but took less time.
	TVD = 1 Recommended	C – Grid	Good solution matches well with default settings.

Special Considerations, Static-Rigid

CGRID: The input file for using the C-grid for an airfoil problem has a couple of key features that should be recognized. First, the dimensioning of the problem needs to be compatible with that established within ensdim.par. Also, it was recognized that breaking the aerodynamic surface into two patches (within FACE 5) is necessary for the static-aeroelastic simulation. Also notice that the interface requires attention.

```
*B.C.'s FOR 1 BLOCK C-GRID
*
BLOCK #1 DEAN's 64A006 WING
*IMAX JMAX KMAX
  261    5   51
FACE.1..IJS..IJE..JKS..JKE..NBC   I=1 PLANE
          1    5    1   51   13
FACE.2..IJS..IJE..JKS..JKE..NBC   I=IMAX PLANE
          1    5    1   51   13
FACE.3..IJS..IJE..JKS..JKE..NBC   J=1 PLANE
          1  261    1   51    9
FACE.4..IJS..IJE..JKS..JKE..NBC   J=JMAX PLANE
          1  261    1   51    9
FACE.5..IJS..IJE..JKS..JKE..NBC   K=1 PLANE
          1   31    1    5    3
         32  131    1    5    1
        131  230    1    5    1
        231  261    1    5    3
FACE.6..IJS..IJE..JKS..JKE..NBC   K=KMAX PLANE
          1  261    1    5   14
 *
```

```
INTERFACES
*ZONE1   PLANE1     INS   INE     INS   INE  ZONE2   PLANE2     INS   INE    INS
INE
     1    K=  1  I=  1    31  J=  1     5      1    K=  1  I=261  231 J=  1
5
END OF SOLVER INPUT
```

O Grid

```
*B.C.'S FOR 1 BLOCK O-GRID
*
BLOCK #1 DEAN's 64A006 WING
*IMAX JMAX KMAX
  201    5   51
FACE.1..IJS..IJE..JKS..JKE..NBC  I=1 PLANE
           1    5    1   51    3
FACE.2..IJS..IJE..JKS..JKE..NBC  I=IMAX PLANE
           1    5    1   51    3
FACE.3..IJS..IJE..JKS..JKE..NBC  J=1 PLANE
           1  201    1   51    9
FACE.4..IJS..IJE..JKS..JKE..NBC  J=JMAX PLANE
           1  201    1   51    9
FACE.5..IJS..IJE..JKS..JKE..NBC  K=1 PLANE
           2  101    1    5    1
         101  200    1    5    1
FACE.6..IJS..IJE..JKS..JKE..NBC  K=KMAX PLANE
           1  201    1    5   14
*
INTERFACES
*ZONE1   PLANE1     INS   INE     INS   INE  ZONE2   PLANE2     INS   INE    INS
INE
     1    I=  1  J=  1     5  K=  1    51      1    I=201  J=  1     5  K=  1
51
END OF SOLVER INPUT
```

H GRID

The H- Grid was done in the standard manner. On note is the use of bc104 to define the surface of the airfoil. Also, please notice the indices for the interface and airfoil surfaces. The leading edge is included in the airfoil, and the trailing edge is included with the interface. This is concurrent with the recommendations in the manual for an Euler solution. The user must also be sure to have the proper dimensioning for the H-Grid. Because there are two blocks, the number of points for H- is larger than for C- or O-.

```
*B.C.'S FOR H-GRID
*
BLOCK #1 H GRID
*IMAX JMAX KMAX
  181    5   51
FACE.1…JS…JE…KS…KE..NBC  I=1 PLANE
           1    5    1   51   12
FACE.2…JS…JE…KS…KE..NBC  I=IMAX PLANE
           1    5    1   51   13
FACE.3…IS…IE…KS…KE..NBC  J=1 PLANE
           1  181    1   51    9
```

```
FACE.4…IS…IE…KS…KE..NBC   J=JMAX PLANE
          1  181    1   51    9

FACE.5…IS…IE…JS…JE..NBC   K=1 PLANE
          1  181    1    5   14
FACE.6…IS…IE…JS…JE..NBC   K=KMAX PLANE
          1   50    1    5    3
         51  150    1    5  104
        151  181    1    5    3
BLOCK #2 H GRID
*IMAX JMAX KMAX
  181    5   51
FACE.1…JS…JE…KS…KE..NBC   I=1 PLANE
          1    5    1   51   12
FACE.2…JS…JE…KS…KE..NBC   I=IMAX PLANE
          1    5    1   51   13
FACE.3…IS…IE…KS…KE..NBC   J=1 PLANE
          1  181    1   51    9
FACE.4…IS…IE…KS…KE..NBC   J=JMAX PLANE
          1  181    1   51    9
FACE.5…IS…IE…JS…JE..NBC   K=1 PLANE
          1   50    1    5    3
         51  150    1    5  104
        151  181    1    5    3
FACE.6…IS…IE…JS…JE..NBC   K=KMAX PLANE
          1  181    1    5   14
*
INTERFACES
*ZONE1   PLANE1     INS   INE     INS   INE ZONE2   PLANE2     INS   INE     INS
INE
     1    K= 51   I=  1    50   J=  1     5      2    K=  1   I=  1    50   J=  1
5
     1    K= 51   I=151   181   J=  1     5      2    K=  1   I=151   181   J=  1
5
*
END OF SOLVER INPUT
```

5.3 ADDITIONAL ALGORITHM OPTIONS

Part of the continued development of ENS3DAE is the addition of optional algorithms and differencing/dissipation schemes. Included in these additions are a 2-factor Lower/Upper Symmetric Gauss Siedel algorithm and Upwind and central differencing schemes using the TVD or flux limited. Closer examination of these options is needed. Results obtained from a preliminary investigation suggest problems with the flux-limiting dissipation scheme with the C-Grid.

5.4 STATIC AEROELASTIC AIRFOIL

Although the improvements to the code ultimately proved successful, other insights were needed to allow for the reasonable simulation of the static aeroelastic problem. The results discussed within were obtained using an initial AOA of 2 degrees. The dynamic pressure was set to 0.03 for the flight condition of 0.87 Mach. With this configuration, a moderate static deflection of the airfoil was achieved on both pitch and plunge.

The most important results of this study are the code modifications and identification of key features within the input file.

The user manual is sufficient in describing the input for structural data for use in the static aeroelastic module with C- and O- grid topologies. However, the shaded regions of the input files for C- and O- grids highlighted above are quite important. Recommendations for changes within the manual are in progress.

Examining the flow solution and generalized displacements, it is clear that some modification should be made to the airfoil geometry before a dynamic aeroelastic run is conducted. Specifically, problems arise with the sharp trailing edge with the O – grid. The small hook that is visible in the dynamic rigid solution causes problems when an angle of attack is applied. Visible in the following figures, the shock position is slightly different in the O- grid. This small problem causes the 4% difference in static vertical displacement visible in figure 11.

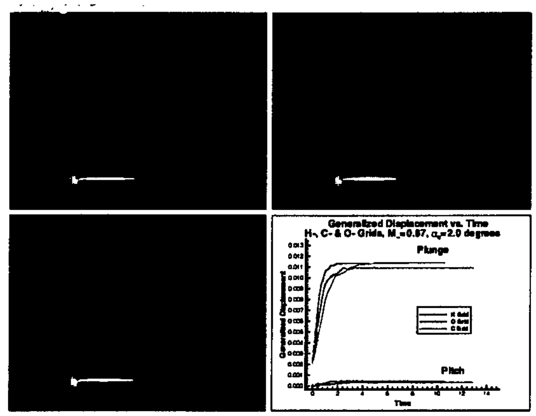

Figure 11. Pressure Field for the Static Aeroelastic Solution. The generalized displacements are also illustrated.

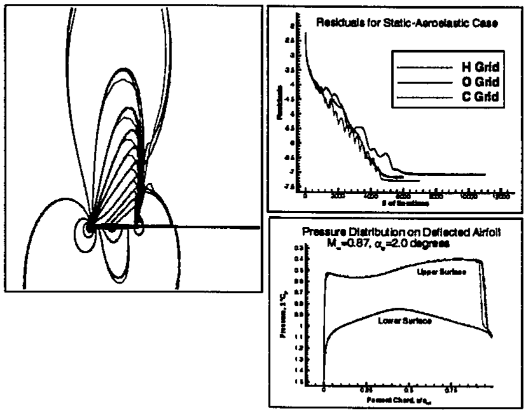

Figure 12. Comparison of the Contour Lines Illustrates the Small Difference in Shock Locations for the O-Grid.

6. Conclusions

Further investigation into this topic before standardized use is clearly needed. The apparent issues regarding the time accurate modules cause great concern. Before conducting the dynamic aeroelastic cases, some resolution is needed.

Additionally, the difficulty getting valuable solutions from the flux-limiting dissipation scheme for the C-grid warrants a close look. The LU-SGS algorithm does perform faster than the standard 3-factor Approximation Factorization scheme, but caution should be exercised. Recommendations have been made to examine this problem.

However, using default settings and recommended values provided by the user manuals, a flow solution is attainable. With current code modifications and input file recommendations, users should be successful in generating a static aeroelastic solution.

As future work, the development of the dynamic aeroelastic solutions to predict flutter speed and LCO characteristics can be done. Also, solution of problems utilizing the 3 dimensional capabilities of ENS3DAE with the C- and O- grids should be investigated.

As mentioned, a co-op student from Iowa State University completed this work. The value of this work as contribution to the industry is up for debate, however, the work proved extremely valuable for personal experience.